Volume 13
Number 14
14 April 2025
Pages 9571–10246

Journal of Materials Chemistry A

Materials for energy and sustainability

rsc.li/materials-a

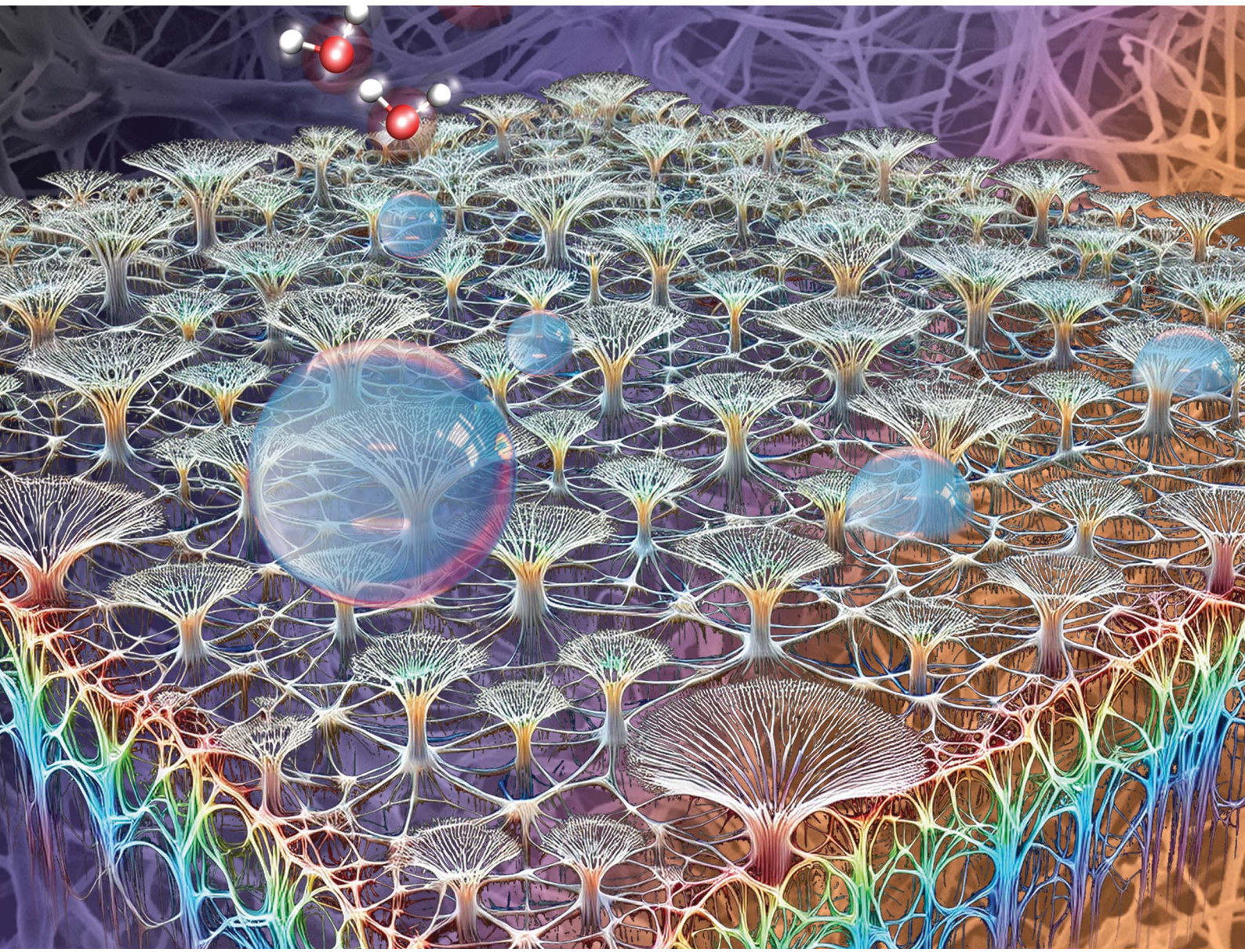

ISSN 2050-7488

ROYAL SOCIETY OF CHEMISTRY

PAPER

Zhao Qin *et al.*

Mycelium–coir-based composites for sustainable building insulation

Journal of Materials Chemistry A

ROYAL SOCIETY OF CHEMISTRY

PAPER

View Article Online
View Journal | View Issue

Cite this: J. Mater. Chem. A, 2025, 13, 9694

Mycelium–coir-based composites for sustainable building insulation†

Gargi De, ‡[ab] Libin Yang,‡[ab] Jaejun Lee, [c] Yu-Han Wu, [c] Zhiting Tian[d] and Zhao Qin *[abe]

Building insulation materials are widely used in building envelopes to improve the energy efficiency of buildings and effectively reduce the energy cost for space cooling and heating. As a result, they contribute to a sixth of the world's total energy consumption and GHG emissions. However, many conventional insulation materials are either energy-intensive or made of petroleum-based plastics, and their production is not sustainable. Here, we focus on fungal biotechnology to produce mycelium–coir-based composites (MCBCs) that are fully derived from biomass with potential application in insulating building envelopes. We inoculated mycelium from simple spores to an integrated network with coir fibers in the form of boards and blocks. MCBCs were found to be good insulators with low thermal conductivity (0.035 ± 0.008 W m^{-1} K^{-1}), similar to polymer foams. We isolated the thin surface film of pure mycelium and measured the thermal conductivity with a laser flash method. An ultralow thermal conductivity of 0.015 ± 0.003 W m^{-1} K^{-1} was identified for *Ganoderma lucidum*, which was lower than the thermal conductivity of pure air, making the film essential for MCBC insulation. Moreover, our series of in-lab tests demonstrated that the composite was more fire-tolerant and hydrophobic than conventional insulation materials, had load-bearing capability similar to polymer foams in compression, and could be further densified to reach optimal specific mechanical functions according to data-driven models. Our study demonstrates that MCBCs are promising materials that may be used to reliably and sustainably improve building insulation functions.

Received 5th November 2024
Accepted 12th February 2025

DOI: 10.1039/d4ta07869a

rsc.li/materials-a

1. Introduction

The construction industry, including manufacturing, delivering, applying, and recycling building materials, accounts for approximately 34% of all global greenhouse gas (GHG) emissions.[1] 45% of such emissions are associated with space cooling and heating (Fig. 1), where insulation within the building envelope plays a crucial role in energy efficiency.[4–9] The building construction industry heavily relies on mineral wool, fiberglass, and extruded polystyrene (XPS) made from synthetic insulation materials.[10] While effective in thermal performance, these materials pose significant environmental challenges. They are often derived from non-renewable resources, involve high energy consumption during production, and are non-biodegradable, contributing to landfill waste at the end of their life cycle. Polymer-based foams can gradually release chemical substances (*e.g.*, formaldehyde, hydrogen cyanide, and VOCs like isocyanates) during operation and disposal, posing health-related risks.[11,12] The high carbon emissions associated with the intensive energy requirements for their production also exacerbate climate change, underlining the urgent need for sustainable alternatives.[13] Among various sustainable materials, insulations derived from biomass, such as mycelium-based composites (MBCs), present a promising alternative.[4–9,14,15] Mycelium, the vegetative part of fungi, can be cultivated from biomass resources to form valuable composite materials.[15,16] These mycelium-based composites offer several advantages, including biodegradability and low embodied carbon, and thus have the potential to be applied to construction to reduce GHG emissions.

Primarily because of their low-energy manufacturing process and utilization of agricultural waste materials, mycelium-based composites offer significant environmental advantages over petroleum-based insulation materials like extruded polystyrene (XPS). The stages involved in the production of mycelium

[a]Laboratory for Multiscale Material Modelling, Syracuse University, 151L Link Hall, Syracuse, NY 13244, USA
[b]Department of Civil and Environmental Engineering, Syracuse University, 151L Link Hall, Syracuse, NY 13244, USA
[c]Department of Materials Science and Engineering, Cornell University, Ithaca, NY 14853, USA
[d]Sibley School of Mechanical and Aerospace Engineering, Cornell University, Ithaca, NY 14853, USA
[e]The BioInspired Institute, Syracuse University, NY 13244, USA. E-mail: zqin02@syr.edu

† Electronic supplementary information (ESI) available. See DOI: https://doi.org/10.1039/d4ta07869a

‡ These authors contributed equally to the work.

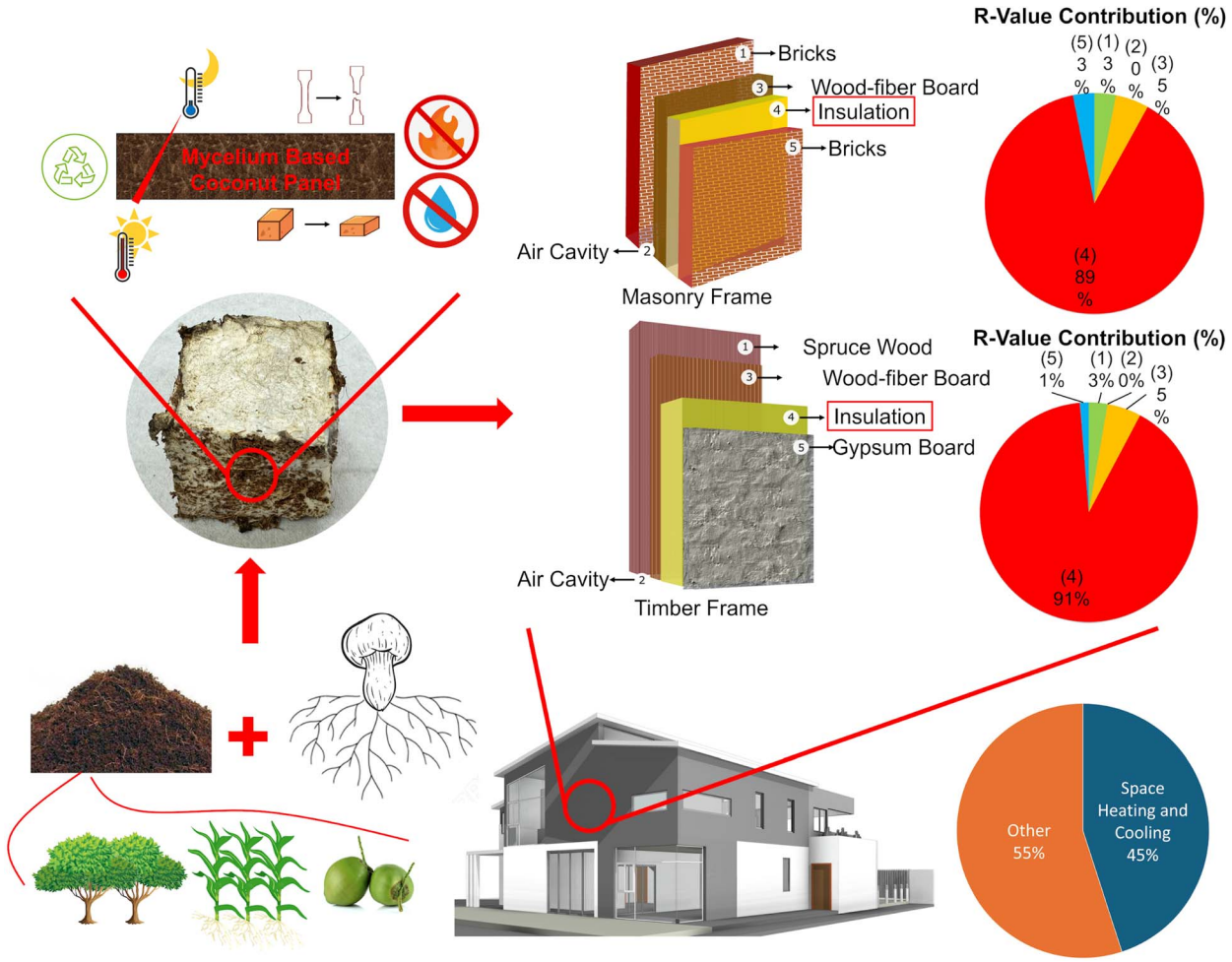

Fig. 1 The application and effectiveness of mycelium–coir-based composite (MCBC) boards as sustainable construction insulation panels. The left part of the figure shows that agricultural biomass (*e.g.*, wood trim, agriculture waste, and coir) combined with mycelium is used to generate MCBCs. We performed various material characterizations to evaluate its functionality. The diagrams on the right compare the thermal resistance (*R*-value) contributions of multiple components within masonry and timber frame constructions, emphasizing the significant impact of the insulation layer on the temperature preservation of buildings.[2] The pie chart at the right-lower corner also shows the energy consumption patterns in buildings, highlighting the potential for improved insulation to save energy, especially in areas like space heating and cooling. On average, the U.S. spends about 45% of its energy on heating and cooling in residential buildings, as shown here.[3]

composites involves fungal growth on substrates such as rye grains,[17] beech sawdust,[18] or hemp[19] under moderate conditions (22–25 °C and 65–90% relative humidity); it is then followed by minimal post-processing, such as heat treatment at 60 °C (ref. 20 and 21) to stop microbial activity. The demand for fossil energy necessitated by following these steps is just 7.7 MJ kg^{-1}, lower than one-tenth that of the 83.5 MJ kg^{-1} required for XPS, which relies heavily on high-temperature polymerization and fossil-derived inputs.[18,19] An examination of the greenhouse gas (GHG) emission during its production shows that mycelium-based composites emit only 0.3668 kg of CO_2 per kilogram of material, which is a 45% reduction in GHG emissions compared to traditional fossil-based insulations.[18,19] Moreover, the transition from the lab-scale to industrial-scale production of fungal-based composite bricks can potentially achieve a further decrease of 68% in climate change impacts.[22] Their ability to sequester carbon during growth and their use of biodegradable, locally available agricultural by-products (such as coir, sawdust or hemp), duly conforming to the circular economy principles, significantly enhance their environmental benefits in large-scale applications.[19] Besides production, we focus on the long-term advantage of MBCs. Life cycle assessment (LCA) studies reveal that MBC panels, when integrated into building envelopes, have the capacity to reduce annual GHG emissions by 72–73.04% compared to uninsulated walls.[17] In fact, the general requirement for building insulation to be incorporated in all constructions is widely distributed throughout the country. Compared to other primary layers, the insulation layer contributes to 89% and 91% thermal resistance of the entire building wall of masonry and timber frame constructions, respectively (Fig. 1).[2,3] The insulation layer thus plays a crucial role in preserving the energy efficiency of buildings by minimizing heat transfer between the interior and exterior environments. It helps maintain stable indoor temperatures,

reducing the need for excessive heating in the winter and cooling in the summer, which is important for indoor comfort and operational energy consumption. Moreover, it can increase the overall lifespan of the building by preventing extreme temperature- and moisture-related damages. The production of synthetic materials relies on equipment, energy supply, and raw materials; thus, it tends to be centralized. However, the output of mycelium-based composites is more flexible as it can use any locally available biomass, including agricultural wastes, tree trims, and coconut coir, without the need for complex reactors, making the decentralized manufacturing of insulation layers possible and reducing the delivery cost. This process broadly repurposes biomass wastes and sequesters carbon, contributing to a circular economy. Such an advantage in production provides another significant advantage over conventional insulation materials.[4,16,23,24]

Here, we study the in-lab composite synthesis by cultivating mycelium on coconut coir as the byproduct of coconut. Early work has shown that mycelium fibers integrate the coir fibers and create a solid, foam-like material that can be used for insulation boards.[2,7] Compared to wood saw dust and agriculture waste, coir has the advantage of material composition, which is rich in lignin. Coconut coir, a lignocellulosic material derived from coconut husks, is primarily composed of cellulose (32–50%), lignin (30–46%), hemicellulose (0.15–15%) and pectin (3–4%).[25] This lignin-rich composition, especially that

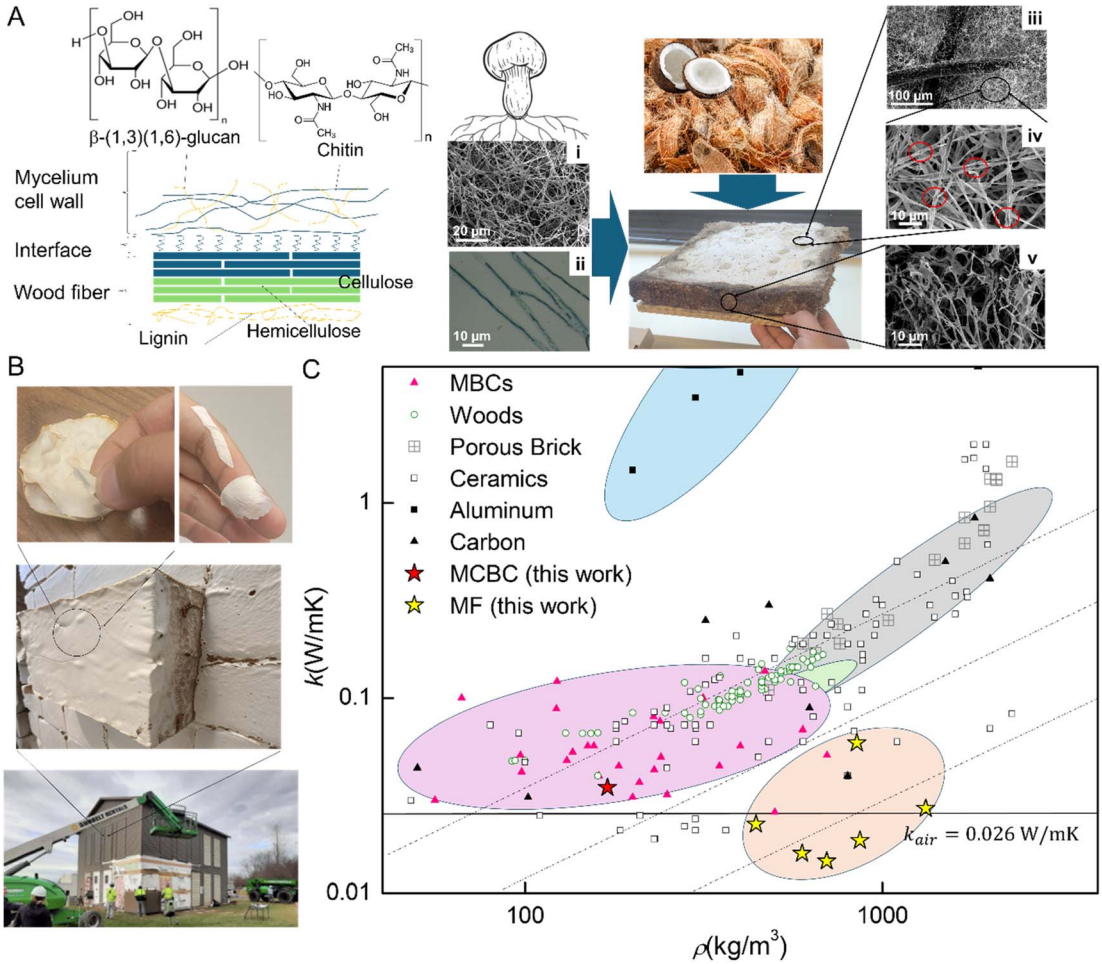

Fig. 2 The multiscale structure of MCBC and its outstanding low thermal conductivity. (A) Schematic of the molecular composition of the cell wall structure of a mycelium fiber and its interface with a wood fiber, snapshots of coir wastes and a picture of a 250 × 250 × 25 mm^3 MCBC board for mid-scale thermal test. (i) The SEM image of the *G. lucidum* mycelium network (scale bar: 20 μm); (ii) the optical image of the *G. lucidum* mycelium after growing for three days and dyed (with a dark blue color dye) before taking the image, showcasing the tubular structure of the mycelial hyphae. The three right images show: (iii) SEM of a sample taken from the surface of the MCBC showcasing the intricate interface between the mycelial hyphae and coconut fibers, highlighting their successful binding mechanism; (iv) zoomed-in SEM image (10 μm scale) illustrating the detailed structure of the mycelial hyphae fully occupying the surface of the MCBC; (v) SEM image of a sample extracted from the core of the MCBC, revealing the inner structure. The image highlights an uneven distribution of mycelium within the MCBC. (B) Picture of the MF film and a visual example of MCBC bricks for a thermal insulation improvement of a building.[30] (C) An Ashby plot of the thermal conductivity (k) of different materials as a function of their material density (ρ) with the data of MBCs collected from various references in the ESI,† the data of woods from a previous study,[31] the data of ceramics, aluminum, and carbon from previous studies,[32,33] and MCBC and MF based on the current study with details summarized in Section 2.3. The thermal conductivity of air in 20 °C is given as k_{air} for reference. The dash lines are parallel with the linear fit of the k–ρ relationship of woods for reference.

found in brown coconut coir (42.2%),[26] contributes to the durability and hydrophobicity of the fibers. The lignin, along with the waxy surface of the fibers, improves the water repellency. The cellulose-rich content enhances the material's strength and flexibility, enabling its extension beyond its elastic limit without failure, while also facilitating bonding with other materials.[26–28] Coir also exhibits low thermal conductivity due to its unique structural and molecular arrangement. Its fibers contain approximately 60% amorphous regions within their structure, which resist vibrational energy, thus lowering thermal conductivity. The absence of an aromatic backbone and cross-linked cellulosic chains also lowers their thermal conduction, as these properties are known to contribute to higher thermal conduction in materials. Morphologically, they are highly porous with one-third of their structure filled with air due to numerous internal cavities and hollow, narrow cells.[29] Since air is a poor conductor of heat, these morphological features improve their thermal insulation capabilities. This positions it as an ideal substrate for MCBCs. We aim to obtain mycelium–coir-based composites (MCBCs) in the forms of boards and blocks (Fig. 2A and B) with comparable thermal resistance to conventional insulation materials (*e.g.*, XPS, with thermal conductivity $k = 0.03$–0.04 W m^{-1} K^{-1} (ref. 6 and 34)) for building envelopes. We started with *Ganoderma lucidum* because it has demonstrated a fast growth speed[35] and degrades the high lignocellulose content within the coir,[36] but we also cultured and tested the thermal function of other mycelium films (MFs). Comprehensive evaluations were conducted to assess its mechanical properties, thermal conductivity, fire resistance on the surface, and interactions with water. These evaluations are crucial for building insulation materials because they ensure that the materials meet various ASTM and ASHRAE standards for safety, performance, and durability over the life of the building.

2. Results and discussions

2.1 Sustainable manufacturing of MCBCs

We used coconut coir as the substrate, and malt and yeast liquid nutrition to support mycelium growth. The multiscale structure of the composite is shown in Fig. 2A, with the fabrication process summarized in Fig. 3A. The coir was hydrated with boiling water to achieve thorough soaking, and autoclaved to eliminate unwanted microorganisms. The autoclaved coir was cooled to room temperature and mixed with liquid nutrition of different levels of concentrations (*i.e.*, high: 240 g per L malt with 120 g per L yeast and low: 160 g per L malt with 80 g per L yeast). The *Ganoderma lucidum* mycelium inoculated within either a solid rye culture or liquid culture was seeded into the coir substrate. The mycelium–coir mixture was in an acrylic box of different sizes (*e.g.*, 250 × 250 × 25 mm^3, 150 × 150 × 50 mm^3, 50 × 50 × 50 mm^3) for shaping purposes. We used a semi-permeable polypropylene bag with a microporous filter patch to inoculate the box and stored the setup in the green tent with constant temperature and humidity (*i.e.*, 24 °C and 90 RH%) for a certain amount of time t_{MCBC} that varied from 2 weeks to 4 months. After the mycelium was allowed to grow for the set time periods, we used a dehydrator (60 °C, 18 hours) to remove the water in the bricks. We named these MCBC samples according to their different inoculation times and preparation conditions (*e.g.*, SLS for $t_{MCBC} = 1$ week, seeding with liquid-culture mycelium and low nutrient concentration, SRS for $t_{MCBC} = 2$ weeks, seeding with rye culture mycelium and low nutrient concentration, LRL for $t_{MCBC} = 2$ weeks, seeding with rye culture mycelium and high nutrient concentration, SRLL for $t_{MCBC} = 4$ months, seeding with rye culture mycelium and high nutrient concentration. See Table S1 in the ESI† for the full name list and details).

Mycelium is tubular in nature, as can be seen in Fig. 2Aii. Its primary composition within the cell wall (*e.g.*, mannan, glucan, chitin, and protein) is rich in charged carbonyl and hydroxyl groups that can form hydrogen bonds with coir fiber (which is mainly composed of cellulose, hemicellulose, and lignin). It can grow within the coir without intense energy inputs. It forms a dense network with the fiber diameter varying from 1.5 to 2.5 μm. The SEM images in Fig. 2Aiii–v show that mycelium fully occupies the surface area, but is not evenly distributed in the inner part of the bio-composite. This idea was further confirmed by the SEM seen in Fig. 2Aiii. The image shows that mycelium entangles and interacts with the coir fibers, indicating that the surface mycelium layer generally contributes to mycelium's good flame-retardant ability. The detailed SEM seen in Fig. 2Aiv shows the compact mycelium fiber and the unique structure of the mycelium clamp connection, allowing us to distinguish the mycelium from the coconut coir, and how fully the surface has been occupied by the mycelium. The SEM in Fig. 2Av shows the inner layer of the mycelium bio-composite, indicating the uneven mycelium distribution compared to the surface and the larger pore size and porosity of the MCBC bio-composite. Even though the core contains less mycelium, the porous structure can still contribute to the thermal resistance ability. We obtained MCBC boards and blocks from mycelium inoculation. We can also peel off the dense MF from the surface of MCBC, rye culture, or agar substrates (Fig. 2B) for characterization. Using a custom-built thermal chamber, we measure the thermal conductivity of the MCBC board and obtain its low value as $k_{MCBC} = 0.035 \pm 0.008$ W m^{-1} K^{-1} (see Section 2.3 and Experimental section for details) with a density of 170 kg m^{-3}. This k_{MCBC} is significant in comparison to most lightweight construction materials (*e.g.*, wood, porous metal, brick, ceramics, and carbon), as well as other known MBCs, as summarized in the Ashby plot[37] in Fig. 2C. This shows that our MCBC board is a promising material for insulation applications, as the low k is crucial for keeping comfortable indoor temperatures, while minimizing energy consumption for heating or cooling. From the Ashby plot, it is shown that conventional construction materials have $k \propto \rho^A$ with a significant A value ($A = 0.6$ for wood, $A = 1.5$ for porous brick, $A = 1.9$ for porous aluminum, $A = 1.3$ for porous carbon, and $A = 0.19$ for porous ceramics). In contrast, the MBCs/MCBC's thermal conductivity weakly depends on the density and $A = 0.04$ by fitting, suggesting that MBCs differ from conventional porous materials with their material properties being far beyond the functions of material density.

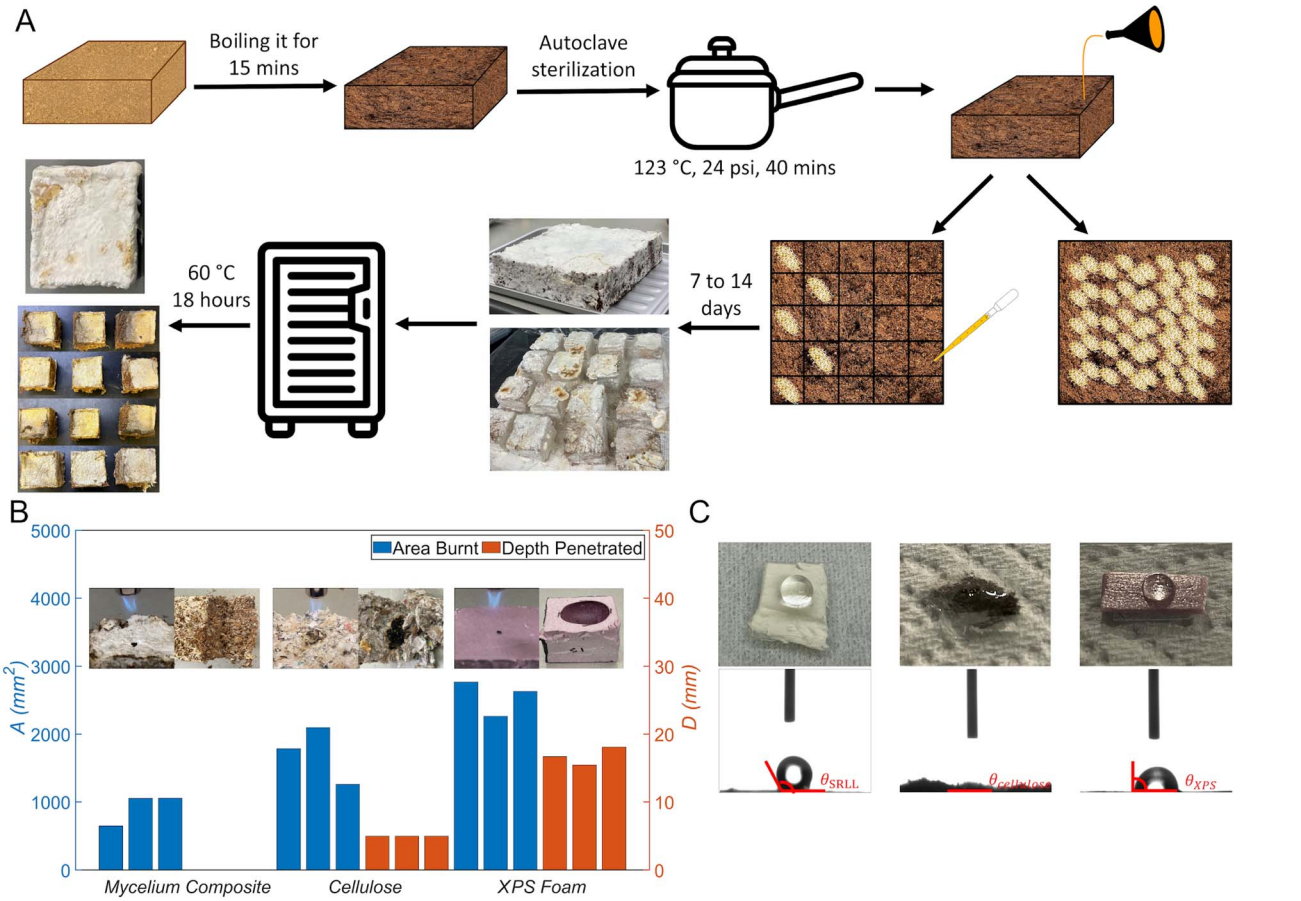

Fig. 3 The preparation process for MCBC boards and blocks and their fire and water resistance. (A) The general process of preparing the MCBC blocks. We used liquid-culture mycelium and rye-cultured mycelium inoculated with coir and nutrient solvent. Different acrylic molds are used to measure the sample size and shape during inoculation. (B) Comparative analysis of the flammability properties of three different materials (three samples each), represented in terms of the area burnt and depth penetrated. The graph illustrates the experimental results for three material categories: MCBC, cellulose insulation, and XPS foam. The blue bars indicate the total area (A) burnt during the test, while the orange bars represent the depth (D) to which the fire penetrated each material. The average spread of areal fire is determined by the average A as 920.0 ± 90.0 mm^2 for MCBC, 1700.0 ± 350.0 mm^2 for cellulose insulation, and 2600.0 ± 210.00 mm^2 for XPS foam during the 40 s test time. Insets show close-up images of each material during and post-burn, highlighting the physical impact of fire exposure. (C) Contact angle tests on three different material samples. The top row displays the initial interaction of water droplets with each material—left to right: MCBC, cellulose insulation, and XPS foam. The lower row images capture the droplet profiles at rest, demonstrating the surfaces' contact angles (θ). These images illustrate the varying hydrophobic properties of each material, with the MCBC showing significant water resistance compared to others.

2.2 Multifunctional MCBCs for fire and water resistance

Flammability testing for insulation materials is crucial toward understanding their fire safety, where the spread of areal fire measurement is essential in assessing the fire performance of the material and quantifying its contribution to the fire hazard in case of ignition. Some insulation, such as fiberglass, is naturally fire-resistant, while others (like foams) may not resist fire effectively.[38] This property is essential in preventing building fires from spreading quickly, potentially saving lives and reducing property damage. Here, we run a preliminary surface flammability test to analyze the surface flammability of MCBCs and compare their performance with some of the existing insulation materials (*i.e.*, cellulose and XPS board). We use the MCBC blocks (50 × 50 × 50 mm^3) as prepared through the SRLL inoculation and dehydration process, as shown in Fig. 3A. We run the test with a windproof butane fire torch following the DIN EN 13501-1 test standard.[39] Three samples of each material were tested. The fire source was positioned approximately 4 cm above the surface of each sample, and the surfaces were exposed to the flame (with a fixed gas flow) for 40 seconds, as can be seen in Fig. 3B. According to the EN standard, this time is sufficient, as materials in classes B, C, and D (low to medium flammability) are tested with a 30-second flame exposure. After exposure, the fire source was removed, and the surface burned area and depth of penetration were measured.

The test results are summarized in Fig. 3B, showing that the SRLL samples exhibited burnt areas of 920 ± 190 mm^2. No ignition or depth penetration was recorded, and MF entirely blocked the fire damage on the MCBC surface. The cellulose samples showed burnt areas of 1700 ± 350 mm^2 with a penetration depth of 5 mm, and ignited upon exposure to the flame. The XPS samples had the largest burnt areas of 2600 ± 210 mm^2 with a penetrated depth of 16.7 ± 1.1 mm, but no ignition. Despite the absence of ignition, the significant burnt area and

depth penetration suggest that SRLL is significantly less flammable and less damaged in burning than cellulose and XPS. The test indicates that MCBC may limit the spread of flames and maintain structural integrity for fire-resistant insulation.

MCBCs are flame-retardant primarily because of the biochemical composition of mycelium. Chitin, a polysaccharide commonly found in fungal cell walls, is a key contributor due to its nitrogen-containing amide functional groups (–CONH–), which promote the formation of a protective char layer in fire. This protective layer is resistant to heat and oxygen, effectively reducing flame spread.[40] Proteins and glucans in mycelium further provide sources of carbonaceous char layer, thereby limiting the direct release of combustible gases and increasing fire resistance. FTIR analysis in the literature has revealed that the thermal decomposition of mycelium releases non-flammable gases—primarily CO_2 and H_2O—during the second stage of mass loss (200–375 °C). These gases dilute flammable volatiles, mitigating flaming combustion and improving fire performance.[40] Literature results of thermogravimetric analysis (TGA) corroborate this with a residual char yield between 15–25% by weight at 600 °C,[20,40] supporting our results for the flame-retardant properties of MCBCs when compared to conventional materials.

According to the current preliminary tests, we cannot conclude the flammability class of MCBCs because of the limited sample size and testing conditions. However, they clearly exhibit char formation and self-extinguishing behavior upon flame removal, which demonstrates their inherent flame-retardant properties. Qualitative burning area and depth comparisons also indicate that the perpendicular flame spread on MCBCs is significantly weaker than that observed in the other two insulation materials tested. However, these initial findings require further validation through standardized testing. Future tests include cone calorimetry for the purpose of evaluating the heat release rate (HRR) (ASTM E1354-99) and limiting oxygen index (LOI) tests (ASTM D2863) to determine the material's flammability threshold. These studies will provide a more comprehensive understanding of the fire-retardant mechanisms in MCBCs and ensure their suitability for fire-sensitive applications.

Water-resistant envelope materials help maintain the long-term performance of building walls, and avoid health hazards like mold growth. Hydrophobicity is crucial, as it enables the insulation material to repel water and prevent moisture-related damage to the indoor environment. Here, we used a standard goniometer to determine the wettability of the MCBC surface at room temperature. This test aimed to assess the surface wettability of the mycelium bio-composite and compare its performance with existing insulation materials. MF samples ($1.25 \times 0.75 \times 0.1$ cm^3) taken from SRLL MCBC sample blocks were collected and taped to microscope glass slides to ensure their relative flatness. We dispensed a deionized water droplet on the sample surfaces and measured the contact angle with a microscope. XPS and cellulose of similar sample sizes were used for comparison. The measurement results, as summarized in Fig. 3C, show that the water contact angle for the SRLL sample is $\theta_{SRLL} = 133°$, indicating a hydrophobic surface.[41] In contrast, our measurement showed $\theta_{XPS} = 89.2°$, agreeing with the literature,[42] suggesting a borderline hydrophobic/hydrophilic property. The cellulose sample exhibited complete wetting, with a $\theta_{cellulose} \sim 0°$, indicating the highest wettability. These results demonstrate that the MCBC sample possesses the highest hydrophobicity, which could be advantageous in applications requiring moisture resistance. We believe that the hydrophobic feature of SRLL is attributed to the rich content of hydrophobin proteins embedded in the mycelium cell walls.[20,43]

Hydrophobins, surface-active proteins secreted by filamentous fungi, self-assemble on the fungal cell wall to form a low-energy barrier that repels water. Their amphiphilic structure creates a hydrophobic layer that significantly enhances water contact angles, as demonstrated in multiple studies where mycelium films exhibited WCAs exceeding 130°.[44,45] This property can be tuned through post-processing, such as conditioning at or above 50 °C.[45] In our MCBCs, dehydrating the material at 60 °C results in a contact angle of 133°, consistent with these findings.

In addition to the biochemical properties conferred by hydrophobins, the micrometric roughness of the mycelial surface, as revealed through AFM in previous literature,[20] further amplifies the hydrophobicity. The fibrous structure traps air pockets between water droplets and the surface, reducing wetting and aligning with the Cassie–Baxter model.[20] This dual mechanism—structural roughness and biochemical hydrophobicity—ensures robust water resistance. The hydrophobic feature of the mycelial film prevents water from entering MCBC, keeping MCBCs dry for building applications.

These features highlight that MCBCs are resistant to absorbing liquid water on their surface, which connects to the durability and erosion control of the building envelope over time. Hydrophobicity is important for erosion control, especially when exposed to rain, groundwater, high humidity, and freeze–thaw cycles. It prevents moisture intrusion and structural damage, mold growth, and deterioration of insulation properties, thus enhancing the durability of buildings. It is also beneficial to pest control, as the dry surfaces are less likely to attract pests such as termites or rodents, which are drawn to damp areas.

Building on this principle, the hydrophobic properties of MCBCs were enhanced through a sandwich inoculation method during production. This method involves placing mycelium spawn layers at the bottom edges and the topmost section of the substrate, ensuring full colonization of all external surfaces with a dense mycelium layer that encapsulates the composite. Such encapsulation allows the mycelium to degrade the majority of coconut coir in these sections, forming a protective layer with inherent hydrophobicity. To validate this, a preliminary experiment was conducted using an MCBC sample placed in a climate chamber at 90% RH for 12 days. The sample's weight increased from 14.14 g to 15.82 g, corresponding to a moisture absorption rate of approximately 11.88% by weight, which is significantly lower than that of bio-based materials. For instance, wood-fiber insulation boards absorb moisture by a percentage of weight ranging from 15% to 122%.[46] This highlights the inherent hydrophobicity of MCBCs, attributed to the mycelium layer, although untreated samples may still require further validation to assess their moisture impact on the

thermal efficiency. Future testing will adhere to standards such as ASTM E96, with additional research into natural hydrophobic coatings to optimize performance in varied environmental conditions.

2.3 MCBCs have low thermal conductivity because of the dense mycelium film

We develop a custom-build mid-scale chamber of (30.5 × 30.5 × 30.5 cm^3) with an Arduino board and common building materials, and use it to measure the thermal resistance of the box wall and several different construction materials (Fig. 4B, see Experimental section for details). Thermal resistance measurements were conducted on MCBC samples produced using the SRLL process with dimensions of 250 × 250 × 25 mm^3. For comparison, thermal resistance measurements were also conducted on basswood, plywood, drywall, and XPS boards. The SRLL board exhibits a thermal resistance of approximately 0.7000 m^2 K W^{-1} or 3.975 ft^2 °F h per BTU (*i.e.*, *R*-value in

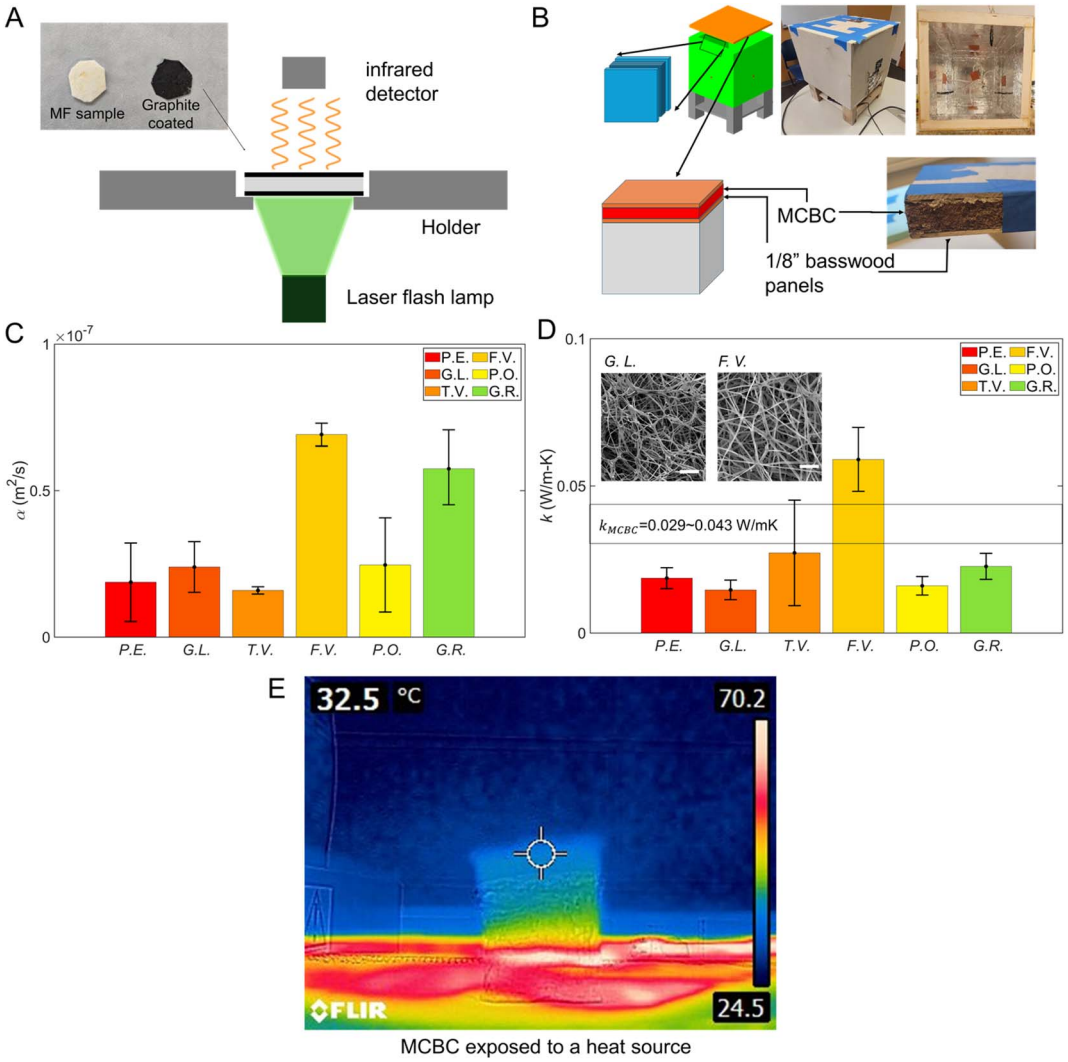

Fig. 4 Characterization of the thermal properties of species of mycelium films (MFs) and MCBC. (A) Schematic of the standard laser flash analysis setup, with the inset figures showing the original and graphite-coated MF samples. (B) Schematic of the setup of the mid-scale chamber and a sandwich structure of the MCBC board sample for thermal measurement. The inset figures show the appearance and inner structure of the chamber, including temperature sensors inside and outside the chamber and heat pads inside the chamber, with the temperature value and the total power consumption of the pads monitored by an Arduino board. (C) The thermal diffusivity (α) of various samples, as measured by laser flash analysis. (D) Thermal conductivity (k) of different MFs of species; *G. lucidum* gives the lowest thermal conductivity, and *F. velutipes* gives the highest k value. The SEM images of their microstructures are inserted for comparison with a scale bar of 20 μm. The dashed line corresponds to the k value of the MCBC boards (0.029–0.043 W m^{-1} K^{-1}), as is measured for the samples shown in panel (B). The equivalent specific thermal resistance is approximately 4.14 ± 0.83 per inch (*R*-value of imperial unit), which is similar to commonly used materials such as the XPS board (*R*-value of 5 per inch). (E) Infrared thermogram of MCBC captured by an FLIR infrared camera, showing the sample exposed to a heat source at approximately 70 °C. A clear temperature gradient across the sample is observed from the thermogram. The highest temperatures indicated by red and yellow tones are observed at the bottom, which is in direct contact with the heat source. Then, there is a transition to moderate temperatures indicated by the green tone and then finally to the upper surface with a much cooler temperature of around 32.5 °C, as indicated by the blue tone.

imperial units; for further data, refer to ESI Table S2 in the ESI†) for a thickness range of 2.03 cm to 3.05 cm. The thickness varies because of the manual synthesis of the plate, which lacks an automation process. The measurement gives a thermal conductivity of 0.029–0.043 W m^{-1} K^{-1} (*i.e.*, specific *R*-value of 3.31–4.97 per inch), which is competitive with XPS boards with k = 0.029 W m^{-1} K^{-1} (*i.e.*, specific *R*-value of 5 per inch). Compared to other building envelope components, we can see that the MCBC outperforms in terms of thermal conductivity; for example, a basswood board ($k = 0.04$ W m^{-1} K^{-1}), a plywood board ($k = 0.038$ W m^{-1} K^{-1}) and a gypsum drywall ($k = 0.044$ W m^{-1} K^{-1}). A lower thermal conductivity generally means the material can provide better insulation within the same wall thickness than others. Our results demonstrate that MCBC provides effective thermal insulation, comparable to traditional insulation materials like XPS boards, and outperforms many construction materials, as is highlighted in Fig. 2C. This makes it a viable alternative for applications requiring thermal insulation, especially where sustainability is prioritized for buildings.

To better understand the mechanism of the low k of MCBCs with accuracy, we collected pure MF samples for six mycelium species (Fig. 2B) by growing and collecting from agar substrates. We measured their thermal conductivity as the product of thermal diffusivity (α), density (ρ), and specific heat capacity (C). The α value for MF samples was measured through a standard laser flash analysis (Fig. 4A) by heating one MF surface with a laser pulse, and measuring the temperature of the other surface infrared detector. The heat capacity was measured using differential scanning calorimetry (DSC). The material density ($\rho = m/d/S$) was calculated by weighing its mass (m) with a scale, and measuring the sample's thickness (d) with a microscope and the area through digital image (S). It should be noted that all measurements are noncontact and were carried out at 20 °C, which prevents the effect of mechanical stress on mechanical deformation, and thus eliminates the impact on the thermal conductivity of a flexible porous media. These properties allow us to calculate how efficiently heat is transferred through the mycelium membranes on the MCBC surface. The measurement results, as summarized in Fig. 4C, show that most mycelium membranes exhibit α in the order of 10^{-8} m^2 s^{-1}, which is significantly lower than typical polymers.[47] At the same time,*F. velutipes* and *G. resinaceum* display a thermal diffusivity that is about three times higher than the others. We believe that the low thermal diffusivity relates to the complex structural feature of mycelium, a collection of μm-scale thin fibers with a hollow core after drying, as a similar thermal management strategy is observed for the hollow polar bear hairs.[48] The density of MFs (Fig. S1B†) is about 1 g cm^{-3}. The heat capacity of MFs is $C \approx$ 0.9 J g^{-1} K^{-1} for all species (Fig. S1A and Table S3, see ESI† for DSC test details). We determined k of MFs, as summarized in Fig. 4D, for different MF samples. The MFs of most species have $k \approx$ 0.02 W m^{-1} K^{-1}, except for *F. velutipes*, which has k = 0.059 W m^{-1} K^{-1}. *G. lucidum* gives the lowest $k = 0.015$ W m^{-1} K^{-1}, which is another reason to use it for MCBCs besides its growth speed. We believe this difference in k relates to the different morphology of mycelium, as *F. velutipes* MF have a uniform fiber diameter (~2.5 μm), with the fibers uniformly distributed and directly connected between the nodes to form an interconnected network. At the same time, *G. lucidum* exhibits a range of fiber diameters (fibers of ~1.5 and ~2.5 μm), with the thicker and thinner fibers entangled (SEM images in Fig. 4D).

It should be noted that these measurements provide one of the most significant results of the study, as it shows that the *G. lucidum* film gives significantly lower thermal conductivity than pure air (k_{air} = 0.026 W m^{-1} K^{-1}). The result suggests that compared to the inner part of the porous media of the mycelium-based composite, which is largely composed of coconut fibers, the top and bottom surfaces of the mycelium-rich layer is more responsible for the thermal resistance of an entire MCBC board. Their low density and porous structures (tube-like structures) create numerous tiny air pockets and traps within and between fibers at different scale levels.[20,34] These air pockets and traps reduce the ability of heat to pass through.

Pure mycelium biomasses of intermediate densities have shown porosities as high as 85%. Even upon increasing the density, their porosity was found to be around 68%.[49] These properties are tunable based on growth media. However, pure mycelium materials have a relatively low achievable thickness for engineering applications, while forming an MCBC board offers good thermal resistance and can be scaled up for practical usage. From this, we can say that the overall low thermal conductivity of MCBC (despite a seemingly higher density of 170 kg m^{-3}) can be attributed to the overall optimized microstructure and material composition. The composites' porosity was calculated from binary segmentation of the material's core's SEM image, as seen in Fig. 2Av, and was found to be around 55.26%. This allows air to be trapped within the pores, influencing the thermal behavior and reducing heat. The SEM analysis reveals a fibrous and irregular framework with thin, elongated features and a random dispersion of fibers, creating a heterogeneous and discontinuous matrix that limits the continuity of heat-conducting pathways and minimizes thermal bridging.

These observed properties of the mycelium–coconut coir composite—high density (170 kg m^{-3}), medium porosity (55.26%), and very low thermal conductivity—are best explained by a combination of Effective Medium Theory (EMT), Phonon scattering theory, and the inherent properties of the materials. EMT suggests that as the material porosity increases, the volume fraction of the conductive phase decreases, thus reducing the effective conductivity of the material.[50] Based on this theory, despite the relatively high density (170 kg m^{-3}), the medium porosity (55.26%) ensures that a significant fraction of air (k_{air} or k_{pore} = 0.026 W m^{-1} K^{-1}) contributes to the composite's low thermal conductivity. Additionally, the pores are irregularly sized and distributed, with smaller pores trapping air and reducing convective heat transfer, and the larger pores disrupting the continuity of the solid matrix. The heat conduction in solids is also attributed to phonons or vibrational energy; the increase in scattering events decreases the material's thermal conductivity.[51] MCBCs with their flexible fibers of a low Young's modulus and irregular microstructure allow these scattering events by introducing multiple interfaces between the fibers and air-filled pores. This random distribution and

discontinuous geometry effectively impede phonon transport, further lowering thermal conductivity.

In comparison with density and thermal conductivity combinations of other bio-based insulation materials, MCBC performs better. A bio-composite insulation material made of cardboard and date palm fibers with densities in the range of 226.6–312.8 kg m^{-3} exhibited thermal conductivities in the range of $k = 0.074$–0.081 W m^{-1} K^{-1}.[52] The MCBC thus achieves a much better density conductivity combination. These findings collectively highlight that the optimized microstructure, rather than density alone, governs the thermal performance of bio-insulation materials. Fig. 4E shows the preliminary infrared thermograms of the MCBCs exposed to a heat source at approximately 70 °C. The red and white tones indicate the high-temperature regions of the source. Meanwhile the MCBC composite (on top) displays a heat gradient transitioning from red/yellow in the lower region, where it is in contact with the heat source, to the cooler green and blue in the upper regions. This transition from hot to cold showcases the ability of the MCBCs to effectively resist heat transfer, essentially maintaining lower temperatures in the upper regions. The uneven heat depicted in the thermograms indicates the MCBC's thermal insulation properties. This temperature gradient is in line with the expected behavior of porous, fibrous materials. The distinction between the hot and cool regions demonstrates their ability to prevent thermal bridging, and the capacity of the composite to limit upward transfer of heat by trapping it in the lower layers.

The MCBC in our study also demonstrates competitive thermal insulation when benchmarked against other bio-based insulation materials tested in the literature, as can be seen in ESI Table S4.† Its performance is better than that shown by flexible hemp batt ($k = 0.040$ W m^{-1} K^{-1}),[53] cellulose fibers ($k = 0.039$–0.041 W m^{-1} K^{-1})[54] and wood-fiber insulation ($k = 0.038$ W m^{-1} K^{-1}).[55] In contrast to eucalyptus bark panels ($k = 0.064$–0.077 W m^{-1} K^{-1})[56] and coconut palm fiber panels ($k = 0.400$ W m^{-1} K^{-1}),[57] the MCBC demonstrates substantially lower thermal conductivity. This positions it as a suitable bio-based insulation material.

2.4 Timing is crucial for strong MCMC production

We performed the compression test on each sample with an Instron machine to understand the effects of different preparations on the mechanical properties of the composite materials. The mechanical deformation of an MCBC block is schematically shown in Fig. 5A, where we include a few snapshots of the block samples before and after the compression test. It is shown that the MCBC blocks were crushed along the loading direction due to a large plastic deformation after the test. Still, there is no significant deformation in the lateral directions, which agrees with many other highly porous media. Fig. 5B summarizes the stress–strain (σ–ε) curves of these MCBC blocks during the compression test (Fig. S2B–D† for MCBC samples prepared for other growth conditions, see ESI† for compression details). It is shown that all of the sample blocks can initially bear the mechanical compression force under a constant engineering strain rate by giving a linear σ–ε curve, but the relationship becomes nonlinear, and the σ increment is slowed down upon reaching a critical yield point. For consistency, we measure the yield strength σ_c using a 0.2% yield

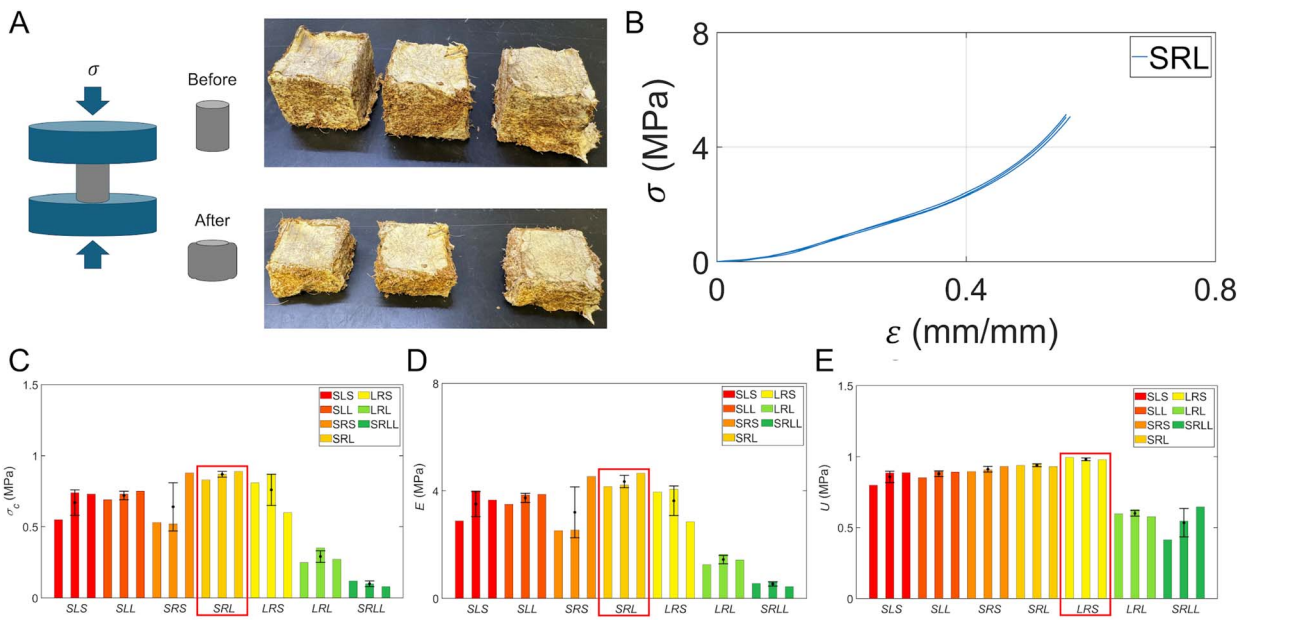

Fig. 5 MCBC samples in mechanical compression tests. (A) Schematic of the compression test under constant loading rate and pictures of the MCBC mechanical samples before and after the mechanical crushing. (B) The stress–strain (σ–ε) curves of MCBC samples that were prepared through an SRL process (Section 2.1 for details). (C) 0.2% yield strength (σ_c), (D) elastic modulus (E), and (E) toughness (U) of samples (SLS, SRL, LRS, SLL, *etc.*) for different growth processes, as summarized in Section 2.1 and Table S1 in the ESI.† It is shown that the mechanical properties of MCBC vary significantly, depending on the preparation conditions. The smaller sample with rye mycelium culture source and higher nutrition concentration growth in a shorter period generally has better mechanical properties than others.

strength criterion for all of the MCBC samples. It is shown in Fig. 5C that the MCBC samples reach the highest strength value of $\sigma_c = 0.87 \pm 0.02$ MPa by inoculation for a period of a week (*i.e.*, $t_{MCBC} = 1$ week) for a high external nutrient content (SRL). In contrast, the samples inoculated under the same condition, but for a longer time, all display an inferior σ_c (*i.e.*, LRL with $\sigma_c = 0.29 \pm 0.04$ MPa for $t_{MCBC} = 2$ weeks, SRLL with $\sigma_c = 0.1 \pm 0.02$ MPa for $t_{MCBC} = 4$ months). It should be noted that MCBC without mycelium is extremely weak in compression test ($\sigma_c \approx 0$ for $t_{MCBC} = 0$). Moreover, for a low external nutrient content, the time for the highest σ_c is delayed to two weeks (*i.e.*, LRS with $\sigma_c = 0.76 \pm 0.12$ MPa for $t_{MCBC} = 2$ weeks) in our tests. Besides the yield strength, we find that a very similar trend takes place for the elastic modulus (E, Fig. 5D) and the modulus of toughness (U, Fig. 5E) in the compression tests, as the samples of one (high nutrient) to two weeks (low nutrient) of inoculation indeed gives higher E and U than other cases. Their highest values are $E = 4.66 \pm 0.23$ MPa for SRL and $U = 0.98 \pm 0.01$ MPa for LRS.

These consistent trends show that mycelium can fully occupy the sample surface within one to two weeks. Their rapid growth can be fully supported by absorbing external nutrients such as malt and yeast added to the coir before inoculation. The nutrients are sufficient to support mycelium growth and integrate the coir fibers without damaging their mechanical strength, leading to high composite strength. The high nutrition concentration at the beginning of the inoculation can accelerate mycelium growth, facilitating network formation and yielding MCBC of high mechanical performance. However, for a more extended growth period, the mycelium starts to degrade the cellulose–lignin structure of coir fibers, which reduces the structural integrity of MCBCs. Another interesting observation is that the MCBC obtained from rye is slightly stronger and tougher than the MCBC obtained from the liquid culture of spores. This is probably because the mycelium from the liquid culture needs more time to grow into robust fibers. Moreover, the highest U is achieved by a group of samples (LRS) different from the group of highest σ_c and E (SRL), suggesting that while a high nutrient content and short amount of inoculation time is essential for σ_c and E, a slightly lower nutrient content and longer time may yield a better-entangled network within the MCBC structure for energy dissipation during loading. Our results suggest that during the preparation of MCBCs for mechanical applications, while all preparing conditions will affect the mechanical performance of the composite, the timing is crucial as the material reaches the optimal mechanics by having high stiffness, strength, and toughness within a relatively short amount of time period. Meanwhile, for longer inoculation, the mycelium starts to digest cellulose and lignin, causing structural damage and weak mechanics of the coir fibers.

2.5 Tunable mechanical functions of MCBCs in heat-press treatment

Although MCBC has shown outstanding thermal resistance, fire tolerance, and hydrophobicity, its mechanical properties with simple dehydration treatment are not impressive, as the few MPa modulus is similar to XPS foam, but it is difficult for structural applications. Here, we investigate how specific mechanics of MCBC (*i.e.*, stiffness, strength, and toughness) can be further improved by densifying the composite. Instead of dehydration after inoculation, we use a heat-press treatment to dry and compress the sample (Fig. S3 for the workflow of sample preparation, see ESI† for sample preparation and tensile test details).

Heat pressing is employed to enhance the alignment and packing density of fibers in the composite, as observed in previous studies on bacterial cellulose films, where the process significantly improved mechanical properties by facilitating strong hydrogen bonding between aligned nanofibrils.[58] Heat pressing was found to be a critical step not only for improving the structural and mechanical properties of fungal mycelium-based materials, but also for modifying their surface structure and chemistry. Additionally, our former study shows that heat pressing influences the chemical composition of the material's surface, enhancing the interactions between fibers and reinforcing the material's mechanical performance for wood and straw substrates.[14] It is shown that heat pressing refines the material's surface and internal structure, ensuring its stability and performance.[20]

However, it is not clear how heat pressing treatment can change the mechanical properties of MCBCs, and we repeat the treatment and mechanical tests as we used in the former study to MCBCs. It should be noted that the heat-press processed samples are only used for mechanical tests, and the composite after heat-press treatments have a much high density are not suitable for thermal insulation. Fig. S4B† summarizes the stress–strain curves of OS samples (explanation of all the abbreviations are in the Fig. S4† caption) in tensile loading (Fig. S2A† for all mutated conditions). It is shown that the samples reach the ultimate tensile strength ($\sigma_U = 12.0 \pm 0.7$ MPa) before the 1% strain, with a Young's modulus of $E = 2400 \pm 430$ MPa, followed by a tail that accounts for energy dissipation during the failure. No significant necking or 45° shear surface is observed at the fracture surface, suggesting brittle failure (Fig. S4A†). Simply from the E value in comparison to MCBCs, we find that the materials after heat-press treatment are two orders of magnitude stiffer.

We discovered that changing the treatment conditions can significantly affect the ultimate strength (σ_U), bulk density (ρ), Young's modulus (E), and modulus of toughness (U) of the samples of reproducibility, as shown by the results summarized in Table S4† for the tensile test outcomes of the sample obtained from different heat-press conditions. Since heat-press treatment also densifies the material, to understand the mechanics-to-weight ratio, we normalize the mechanical outputs by the material density, as the specific strength $\left(\frac{\sigma_U}{\rho}\right)$, specific modulus $\left(\frac{E}{\rho}\right)$ and specific toughness $\left(\frac{U_t}{\rho}\right)$ as summarized in Fig. S4C–E,† respectively. The highlighted red sections show that OS gives the maximum specific ultimate stress $\frac{\sigma_t}{\rho} = 8.67 \pm 0.39$ J g^{-1} (Fig. S4C†), and OT gives the maximum average specific toughness $\frac{U_t}{\rho} = 0.040 \pm 0.012$ J g^{-1}

(Fig. S4E†), conforming with machine learning results. Moreover, the OS samples also display the highest Young's modulus $\frac{E}{\rho} = 1900 \pm 270$ J g^{-1} (Fig. S4D†), which is still two orders of magnitude higher than the specific modulus of MCBC without heat-press treatment. The samples made according to the mutated treatment conditions (OS$t/p \pm 50$ and OT$t/p + 50$) yield lower average specific ultimate strength and average specific toughness. This suggests that neither an increase nor decrease in heat-press treatment time or pressure from OT conditions can yield a better specific toughness. This outcome agrees with the machine learning model's predictions that OT is the saddle point for maximum specific toughness within the temperature–pressure–time space. Similarly, OS is the saddle point for maximum specific ultimate strength within the temperature–pressure–time space. The treatment time and pressure can affect both fiber packing and fiber strength. The long baking time or higher pressure can solidify the composite, but simultaneously make the individual fibers brittle and even rupture for overtreatment, thus decreasing the specific mechanical functions of the composite.

3. Conclusion

The findings of this study highlight the substantial potential of MCBC as a sustainable alternative for building insulation. Its mechanical–thermal performance is comparable to conventional materials, such as XPS and blown-in cellulose insulation. The stiffness and density of MCBC are measured to be similar to XPS foam, ensuring that it can be easily delivered and utilized with a simple utility knife. We find that the low thermal conductivity of MCBC is mainly because of the ultralow thermal conductivity of the MF on the composite surface. This thermal conductivity is even lower than that of air, mainly because of the porous structure and hollow mycelium fibers. Moreover, we find this MF layer is crucial for the superior fire resistance of the MCBCs, which have burnt areas and depth penetration significantly smaller than the other flammable insulations. This MF surface is also hydrophobic, which is critical for resisting liquid water, preventing mold and humid intrusion, and thus ensuring the performance of the building envelope over time.

Based on the lab-scale study, we are collaborating with others to scale up the mycelium-based boards to larger panel sizes to ensure a representative sample for materials with non-uniform properties to replicate real-life installation conditions in order to capture accurate performance data. Although there is limited research on the practical service life verification of such materials, two aspects of these materials affirm that, over time, despite being made of degradable biomass, these materials have the potential to be shelf-stable. Firstly, the hydrophobic nature of mycelium composites enhances their shelf stability by reducing moisture absorption, which is crucial for maintaining insulation performance. Secondly, mycelium-based composites have already demonstrated selective antimicrobial properties. These properties reduce the activity of harmful microorganisms such as viruses and *Staphylococcus aureus*, reinforcing the indoor environment as insulation materials.[59]

Using coconut coir as a natural fiber source, our study demonstrates that MCBC can effectively enhance the sustainability of building material production by repurposing biomass and reducing reliance on energy-intensive manufacturing and non-renewable resources. Because the production of MBCs is not limited to a specific biomass source, nor certain equipment or energy source, their manufacturing will not be geographically limited. This will allow them to be produced through a widely distributed network of fabrication facilities that use waste natural biomass, tap into green energy grids and supply chains of building materials, hopefully create job opportunities in economically disadvantaged regions and reduce delivery cost. Moreover, MCBCs have no additives, making them biodegradable and able to enrich the soil at the end of their life. From raw material to production, delivery, and waste, MCBCs have exhibited significant environmental benefits, as another outstanding material feature beyond their physical properties aligns with global sustainability goals and the growing demand for eco-friendly building solutions.

Our work illustrates that MCBCs present feasible insulation materials for sustainable construction. Their advanced thermal-mechanical functions and environmental benefits are more significant than conventional thermal insulations. Future research should focus on optimizing the cultivation parameters and processing techniques to form recipes for inoculating MBCs with different material sources. These recipes will create a database that enables the production of MBCs of optimal material functions and explore large-scale production methods to facilitate broader adoption in the construction industry. The unique integration of experimental trials and advanced physical and data-driven modeling methods will provide a feasible way to solve this complex engineering problem of high degrees of freedom. For example, our current work demonstrates that MCBCs can be further densified through a machine-learning-guided heat-press process to elevate their stiffness by two orders of magnitudes, enabling their use for some light-duty structural applications. More complex industrial treatments (such as bleaching, etching, and oxidation) can further change the multiscale structure of MBCs from chemical composition to continuum mechanics, and their tunable material functions can be evaluated by the integrated methods as mentioned. By leveraging the unique properties of mycelium-based composites, we can significantly reduce the carbon footprint of building materials and contribute to a more sustainably built environment.

4. Experimental section

4.1 Liquid culture and rye culture preparation

Liquid culture of six species of mycelium, which include king oyster (*P. eryngii*), red reishi (*G. lucidum*), turkey tail (*T. versicolor*), oyster mushroom (*P. ostreatus*), reishi (*G. resinaceum*) and velvet shank (*F. velutipes*.) purchased from the online store, North Spore. Rye is thoroughly washed and soaked in water for a specified period to hydrate, after which they are boiled and steamed to achieve sterilization, eliminating unwanted microorganisms. The sterilized rye grains are then evenly dispersed into glass jars. We put one layer of rye and some small pieces of

mycelium cultured on an agar plate to mix them. Each jar lid is installed with a filter of polytetrafluoroethylene 0.22 μm that allows for gas exchange, while preventing the entry of contaminants. The inoculated jars are then stored in a green tent under dark conditions, where the temperature and humidity are 24 °C and 98 RH% to facilitate the mycelium colonization for over a week until white mycelium is fully grown over the rye particles to form the rye culture. To prepare MCBC with the rye culture, we uniformly seed 3 g cultured material for a $50 \times 50 \times 50$ mm^3 sample. For seeding with liquid culture, we spray 3 mL of cultured material. The amount of seeding materials for larger samples is scaled by volume.

4.2 Flammability test

A preliminary surface flammability test is conducted using a windproof butane fire source based on the DIN EN 13501-1 test standard.[39] Three samples of each material were tested. According to the EN standard, different flaming durations are used to classify materials into various flammability classes. Materials in classes B, C, and D (low to medium flammability) are tested with a 30-second flame exposure, while class E (high flammability) uses a 15-second flame exposure. After dehydration, the $50 \times 50 \times 50$ mm^3 SRLL samples were used to test the surface flammability of MCBC. XPS rigid foam board insulation and cellulose blown-in insulation were obtained from the local store, and were shaped into samples of the same size for comparison. XPS is directly cut to the size. Cellulose cubes were prepared by packing the insulation flakes layer by layer in a cubic mold. Water is added to bind the material together. The cubes are then dehydrated before testing.

4.3 Water contact angle measurements

A Rame-Hart Model 250 Standard Goniometer was used to determine the wettability of the prepared samples. The experiment is carried out at room temperature. Samples are taped to microscope glass slides, ensuring relative flatness and 4 μL deionized water droplets are dispensed on the sample surfaces. The contact angle is then measured using the Instrument DropImage Advanced software with an optical microscope. The SRLL samples are used to test the wettability of mycelium insulation materials. XPS rigid foam board insulation and cellulose blown-in insulation are selected for comparison. For each type of material, thin sample slice ($1.25 \times 0.75 \times 0.1$ cm^3) pieces are used. Sandpaper was used to glue on the base of each sample to ensure approximate uniformity of the thickness of each sample. For the SRLL and XPS samples, the pieces are taken from the top surface of the bulk materials. A small sample of approximately similar size was selected for the cellulose insulation.

4.4 Mid-scale chamber for MCBC thermal resistance measurement

A custom-built mid-scale chamber of ($30.5 \times 30.5 \times 30.5$ cm^3) was built to measure the thermal resistance of the MCBC boards. The chamber consists of wood boards with XPS sandwiched in between. The inner space of the chamber is heated using heat pads (of 30 watts at 12 volts), with the power supplied to these pads measured by monitoring the voltage ($V(t)$) and current ($I(t)$) as functions of time (t) using an Arduino system (data in Fig. S5†). The Arduino also recorded data from three temperature sensors placed inside the chamber (*i.e.*, $T_{i,1}$, $T_{i,2}$, and $T_{i,3}$) and three sensors outside (*i.e.*, $T_{o,1}$, $T_{o,2}$, and $T_{o,3}$), focusing primarily on the top surface of the insulation board. The sides of the chamber are symmetric, thus reducing the need for additional sensors. The system can reach thermal equilibrium within one hour, and then the temperature readings from the sensors were used to calculate the heat flux and temperature difference. Arduino was used to log all the measurements at a 0.5 Hz scanning rate, ensuring the data were accurate and consistent over the 15-hour test period conducted at night when the room temperature remained stable. We first measured the average thermal resistance of the entire cubic box (R_{box}) homogeneously made of six plywood-XPS-plywood sandwich plates *via*:

$$R_{box} = \frac{6A\int_0^t \overline{\Delta T(t)}\,dt}{\int_0^t I(t)V(t)\,dt} \quad (1)$$

where A is the surface area of each box panel and $\overline{\Delta T(t)} = \frac{1}{3}(T_{i,1} + T_{i,2} + T_{i,3} - T_{o,1} - T_{o,2} - T_{o,3})$ is the mean temperature difference between the inside and outside of the box. The top plate is thereafter removed and replaced by different sample materials. This setup allowed for precise calculation of the thermal resistance R_{sample}.

$$R_{sample} = \frac{A\int_0^t \overline{\Delta T(t)}\,dt}{\int_0^t I(t)V(t)\,dt - \frac{5A\int_0^t \overline{\Delta T(t)}\,dt}{R_{box}}} \quad (2)$$

4.5 MF preparation, thermal conductivity, and density measurement

We inoculated all six mycelium species on the agar plate, and put them into the climate chamber for 7–14 days until it fully covered the plate to get the dry mycelium membranes. We used a dehydrator (60 °C and 4 hours) to fully remove the water from all of the samples. The mycelium membrane can be easily torn off from the dry agar substrate (Fig. 2B). All the MF samples are tailored into a 12.7 mm diameter disk shape for thermal tests. The MF sample's thermal conductivity (k) is determined through the following equation:

$$k = \alpha \times C \times \rho \quad (3)$$

where α is the thermal diffusivity, C is the heat capacity, and ρ is the density. To get a more accurate sample thickness, we place the mycelium vertically next to a stack of paper of similar height, and then we use the microscope to take pictures to record the mycelium. We use ImageJ software to measure the thickness (d) of the mycelium membrane. We measure the sample area (S) through a digital image of each sample. The material density ($\rho = m/d/S$) was calculated by weighing its mass (m) with a scale, and measuring the sample's thickness (d) with a microscope and the area through digital image (S).

4.6 Thermal diffusivity by laser flash analysis

The laser flash analysis *via* Linseis XFA 500 is used for thermal diffusivity measurements. The Linseis XFA 500 uses a xenon flash to heat the sample from one end with a controlled energy pulse. A high-speed infrared detector measures the temperature increase at the opposite surface. We recorded the temperature rise curve over time, showing the sample temperature change caused by the xenon flash. By applying mathematical models and known parameters, this method calculates the thermal diffusivity, providing essential information about the thermal properties of the materials over various temperature ranges. MF samples were graphite spray-coated on both sides of the tailored samples to minimize pulse reflection (Fig. 3A). They were mounted on the sample holder and the thermal diffusivity was measured at 20 °C (room temperature). The thermal diffusivity values were obtained by fitting a mathematical model to the time (ms) *versus* temperature rise (volts). The measurements were conducted 3 to 5 times per sample for consistency.

Data availability

The data supporting this article have been included as part of the ESI.†

Author contributions

Z. Q. proposed, designed, and supervised the study. L. Y., G. D., and Z.Q. designed and carried out the preparation experiments on the MCBC samples. L. Y., J. L., Y. H. W., and Z. T. contributed to the thermal conductivity testing and analysis of MFs. Z. Q. designed and built the mid-scale chamber to measure the thermal conductivity of the MCBC boards. L. Y., G. D., and Z. Q. collected the experimental characterization data, analyzed the outcomes, and wrote the paper draft. L. Y. and G. D. contributed equally to the experimental work. All authors commented on and approved the final manuscript.

Conflicts of interest

The authors declare no conflict of interest.

Acknowledgements

L. Y., G. D., and Z. Q. acknowledge the support of the National Science Foundation, USA (NSF Career, Grant# CMMI-2145392). We acknowledge the help of Prof. David G. Chandler from Syracuse University in sharing the space and FLIR thermal camera for characterization. We acknowledge the useful discussion with Prof. Nina Wilson, Prof. Bing Dong and Prof. Jianshun Zhang from Syracuse University

References

1 I. Hamilton, H. Kennard, O. Rapf, J. Kockat, S. Zuhaib, Z. Toth, M. Barrett, C. Milne, C. Delmastro, Y. Monschauer, C. Camarasa, R. Martinez Gordon, I. Bouattay, I. Ben Othmane, O. Wanas, A. Dyson, M. Lokko, A. Mohamed, N. Keena, K. Scrivener, H. Hafez, J. Duwyn, P. Guerecheau, N. Steurer and Y. Cui, *2022 Global Status Report for Buildings and Construction: Towards a Zero-emission, Efficient and Resilient Buildings and Construction Sector*, United Nations Environment Programme, 2022.
2 C. H. Koh, F. Gauvin, K. Schollbach and H. J. H. Brouwers, *Constr. Build. Mater.*, 2022, **346**, 128440.
3 X. Cao, X. Dai and J. Liu, *Energy Build.*, 2016, **128**, 198.
4 D. Alemu, M. Tafesse and A. K. Mondal, *Int. J. Biomater.*, 2022, **2022**, 8401528.
5 X. Zhang, J. Hu, X. Fan and X. Yu, *J. Cleaner Prod.*, 2022, **342**, 130784.
6 Y. Xing, M. Brewer, H. El-Gharabawy, G. Griffith and P. Jones, *IOP Conf. Ser.: Earth Environ. Sci.*, 2018, **121**(2), 022032.
7 P. P. Dias, L. B. Jayasinghe and D. Waldmann, *Results Mater.*, 2021, **10**, 100189.
8 P. M. Velasco, M. P. M. Ortiz, M. A. M. Giro, M. C. J. Castelló and L. M. Velasco, *Energy Build.*, 2014, **80**, 17.
9 E. D. Gezer and S. Kuştaş, *BioResources*, 2024, **19**, 1348.
10 S. Schiavoni, F. D′Alessandro, F. Bianchi and F. Asdrubali, *Renewable Sustainable Energy Rev.*, 2016, **62**, 988.
11 B. Abu-Jdayil, A.-H. Mourad, W. Hittini, M. Hassan and S. Hameedi, *Constr. Build. Mater.*, 2019, **214**, 709.
12 B. P. Jelle, *Energy Build.*, 2011, **43**, 2549.
13 F. Du, W. Zhu, R. Yang, Y. Zhang, J. Wang, W. Li, W. Zuo, L. Zhang, L. Chen, W. She and T. Li, *Adv. Sci.*, 2023, **10**, 2300340.
14 L. Yang and Z. Qin, *Cell Rep. Phys. Sci.*, 2023, **4**, 101424.
15 M. Jones, A. Mautner, S. Luenco, A. Bismarck and S. John, *Mater. Des.*, 2020, **187**, 108397.
16 K. K. Alaneme, J. U. Anaele, T. M. Oke, S. A. Kareem, M. Adediran, O. A. Ajibuwa and Y. O. Anabaranze, *Alexandria Eng. J.*, 2023, **83**, 234.
17 M. Fellah, S. Ouhaibi, N. Belouaggadia, K. Mansouri and H. Naji, *Case Stud. Constr. Mater.*, 2024, **20**, e02786.
18 N. Alaux, H. Vašatko, D. Maierhofer, M. R. Mendes Saade, M. Stavric and A. Passer, *Int. J. Life Cycle Assess.*, 2024, **29**, 255–272.
19 R. Volk, M. Schröter, N. Saeidi, S. Steffl, A. Javadian, D. E. Hebel and F. Schultmann, *Resour., Conserv. Recycl.*, 2024, **205**, 107579.
20 M. Haneef, L. Ceseracciu, C. Canale, I. S. Bayer, J. A. Heredia-Guerrero and A. Athanassiou, *Sci. Rep.*, 2017, **7**, 41292.
21 N. Attias, O. Danai, E. Tarazi, I. Pereman and Y. J. Grobman, *Des. J.*, 2019, **22**, 1647.
22 L. Stelzer, F. Hoberg, V. Bach, B. Schmidt, S. Pfeiffer, V. Meyer and M. Finkbeiner, *Sustainability*, 2021, **13**, 11573.
23 H. Schritt, S. Vidi and D. Pleissner, *J. Cleaner Prod.*, 2021, **313**, 127910.
24 E. Elsacker, S. Vandelook, J. Brancart, E. Peeters and L. De Laet, *PLoS One*, 2019, **14**, e0213954.
25 Y. Guo, P. Tataranni and C. Sangiorgi, *Constr. Build. Mater.*, 2023, **390**, 131754.
26 W. Stelte, S. T. Barsberg, C. Clemons, J. P. S. Morais, M. F. Rosa and A. R. Sanadi, *Waste Biomass Valorization*, 2018, **9**, 1351–1359.

27 I. A. Dewi, A. Ihwah, H. Y. Setyawan, A. A. N. Kurniasari and A. Ulfah, *IOP Conf. Ser.: Earth Environ. Sci.*, 2021, **733**, 012034.
28 F. Gauvin, V. Tsao, J. Vette and H. J. H. Brouwers, *Constr. Technol. Archit.*, 2022, **1**, 643–651.
29 M. A. Mahmud, N. Abir, F. R. Anannya, A. N. Khan, A. N. M. M. Rahman and N. Jamine, *Heliyon*, 2023, **9**, e15597.
30 Y. Jin, G. De, N. Wilson, Z. Qin and B. Dong, *Energy Built Environ.*, 2025, DOI: **10.1016/j.enbenv.2025.01.004**.
31 W. P. Goss and R. G. Miller, Thermal properties of wood and wood products, in *Proceedings of the Thermal Performance of the Exterior Envelopes of Whole Buildings International Conference*, 1992, vol. 28, pp. 193–203.
32 *MatWeb: Online Materials Information Resource*, can be found under **https://www.matweb.com/**.
33 C. Chen, Y. Zhou, W. Xie, T. Meng, X. Zhao, Z. Pang, Q. Chen, D. Liu, R. Wang, V. Yang, H. Zhang, H. Xie, U. H. Leiste, W. L. Fourney, S. He, Z. Cai, Z. Ma, T. Li and L. Hu, *Adv. Funct. Mater.*, 2023, **33**, 2204219.
34 S. Al-Qahtani, M. Koç and R. J. Isaifan, *Sustainability*, 2023, **15**(17), 13217.
35 L. Yang, X. Hu and Z. Qin, *MRS Bull.*, 2024, **49**(12), 1205–1216.
36 H. Bui, N. Sebaibi, M. Boutouil and D. Levacher, *Fibers*, 2020, **8**(6), 37.
37 L. J. Gibson and M. F. Ashby, *Proc. R. Soc. London*, 1982, **A382**, 43.
38 A. Michel Murillo, G. Valery Abisambra, P. Aura Acosta, Q. Claudia Quesada, B. F. Tutikian and H. Z. Ehrenbring, *J. Mater. Res. Technol.*, 2021, **12**, 1958.
39 B. Schmidt, C. Freidank-Pohl, J. Zillessen, L. Stelzer, T. N. Guitar, C. Lühr, H. Müller, F. Zhang, J. U. Hammel, H. Briesen, S. Jung, H.-J. Gusovius and V. Meyer, *Fungal Biol. Biotechnol.*, 2023, **10**, 22.
40 M. Jones, T. Bhat, E. Kandare, A. Thomas, P. Joseph, C. Dekiwadia, R. Yuen, S. John, J. Ma and C.-H. Wang, *Sci. Rep.*, 2018, **8**, 17583.
41 S. Kim, Z. Wu, E. Esmaili, J. J. Dombroskie and S. Jung, *Proc. Natl. Acad. Sci. U. S. A.*, 2020, **117**, 13901.
42 M. L. M. Budlayan, J. N. Patricio, J. P. Lagare-Oracion, S. D. Arco, A. C. Alguno, A. Basilio, F. S. Latayada and R. Y. Capangpangan, *J. Eng. Appl. Sci.*, 2021, **68**, 25.
43 F. V. W. Appels, J. Dijksterhuis, C. E. Lukasiewicz, K. M. B. Jansen, H. A. B. Wösten and P. Krijgsheld, *Sci. Rep.*, 2018, **8**, 4703.
44 M. S. Grunér, G. R. Szilvay, M. Berglin, M. Lienemann, P. Laaksonen and M. B. Linder, *Langmuir*, 2012, **28**, 4293–4300.
45 W. Sun, M. Tajvidi, C. G. Hunt and C. Howell, *ACS Appl. Bio Mater.*, 2021, **4**, 1015–1022.
46 J. Snow, B. Herzog, L. O'Brien and L. Li, *BioResources*, 2024, **19**, 6142–6159.
47 D. S. Smith, A. Alzina, J. Bourret, B. Nait-Ali, F. Pennec, N. Tessier-Doyen, K. Otsu, H. Matsubara, P. Elser and U. T. Gonzenbach, *J. Mater. Res.*, 2013, **28**, 2260.
48 Y. Cui, H. Gong, Y. Wang, D. Li and H. Bai, *Adv. Mater.*, 2018, **30**, 1706807.
49 M. E. Antinori, L. Ceseracciu, G. Mancini, J. A. Heredia-Guerrero and A. Athanassiou, *ACS Appl. Bio Mater.*, 2020, **3**, 1044–1051.
50 L. Gong, Y. Wang, X. Cheng, R. Zhang and H. Zhang, *Int. J. Heat Mass Transfer*, 2014, **68**, 295–298.
51 Z. Guo, Z. Han, D. Feng, G. Lin and X. Ruan, *npj Comput. Mater.*, 2024, **10**, 31.
52 A. Benallel, A. Tilioua and M. Garoum, *J. Cleaner Prod.*, 2024, **434**, 139995.
53 C. Lafond and P. Blanchet, *Buildings*, 2020, **10**, 81.
54 M. Reif, J. Zach and J. Hroudová, *Procedia Eng.*, 2016, **151**, 368–374.
55 O. Ranefjärd, P. B. Strandberg-de Bruijn and L. Wadsö, *Materials*, 2024, **17**, 2021.
56 C. Fuentealba, C. Segovia, M. Pradena-Miquel and A. G. César, *Forests*, 2024, **15**, 1628.
57 D. S. Mededji, E. Sogbochi, A. A. Djossou, O. Cherkaoui, L. A. Fagbemi and D. C. K. Sohounhloue, *Int. J. Environ. Clim. Change*, 2024, **14**, 324.
58 S. Wang, T. Li, C. Chen, W. Kong, S. Zhu, J. Dai, A. J. Diaz, E. Hitz, S. D. Solares, T. Li and L. Hu, *Adv. Funct. Mater.*, 2018, **28**, 1707491.
59 P. Amstislavski, T. Pöhler, A. Valtonen, L. Wikström, A. Harlin, S. Salo, P. Jetsu and G. R. Szilvay, *Cellulose*, 2024, **31**, 8769–8785.